Stabilization of the Resistive Wall Mode by a Rotating Solid Conductor

C. Paz-Soldan, M. I. Brookhart, A. T. Eckhart, D. A. Hannum, C. C. Hegna, J. S. Sarff, and C. B. Forest

Phys. Rev. Lett. **107**, 245001 — Published 5 December 2011

DOI: 10.1103/PhysRevLett.107.245001

Stabilization of the Resistive Wall Mode by a Rotating Solid Conductor

C. Paz-Soldan,* M.I. Brookhart, A.T. Eckhart, D.A. Hannum, C.C. Hegna, J.S. Sarff, and C.B. Forest

Physics Department, University of Wisconsin-Madison, Madison, Wisconsin

Abstract

Stabilization of the resistive wall mode (RWM) by high-speed differentially rotating conducting walls is demonstrated in the laboratory. To observe stabilization intrinsic azimuthal plasma rotation must be braked with error fields. Above a critical error field the RWM frequency discontinuously slows (locks) and fast growth subsequently occurs. Wall rotation is found to reduce the locked RWM saturated amplitude and growth rate, with both static (vacuum vessel) wall locked and slowly rotating RWMs observed depending on the alignment of wall to plasma rotation. At high wall rotation RWM onset is found to occur at larger plasma currents, thus increasing the RWM-stable operation window.

The Resistive Wall Mode (RWM) is a performance-limiting magneto-hydrodynamic (MHD) instability common to many magnetic confinement configurations [1]. It occurs when stabilizing eddy currents in a conducting wall ohmically dissipate, allowing the RWM to grow on the time scale of the wall's resistive diffusion ($\tau_w \equiv \mu_0 \sigma_w r_w \delta_w$, where σ_w, r_w and δ_w are the wall conductivity, radius, and thickness, respectively). It is known that plasma rotation is able to stabilize the RWM [2] as stabilizing eddy currents are inductively regenerated by the moving plasma. Analagously, theory suggests [3–6] that a system of differentially rotating conducting walls can stabilize the RWM, as the RWM will always be rotating in the frame of one of the two walls. RWM stabilization has been previously achieved both by active drive of plasma rotation [7] and the use of active feedback coils [8–10], though next-step devices will be limited in their ability to drive plasma rotation [11]. Stabilization by physically moving conductors is of further interest due to its analogy to an infinite set of active coils [12], the predicted robustness of stabilization [6], and the application to future devices utilizing flowing liquid metals for cooling, tritium breeding, or the first wall [13].

In this Letter it is shown for the first time that a physically rotating conducting wall can successfully stabilize the RWM. Intrinsic plasma rotation yields a kHz-scale rotating RWM which must be braked to observe the interaction of the instability with the rotating wall. For sufficiently braked (locked) modes, wall rotation is found to reduce the RWM growth rate, saturated amplitude, and to extend the RWM-stable operation window.

Experiments are performed on the Rotating Wall Machine [14], a 1.2 m long by 16 cm diameter screw-pinch shown in Fig. 1. A uniform 500 G axial guide field (B_z) is applied by four external solenoids and azimuthal field is provided by up to 7 kA of plasma current (I_p). Plasmas are generated by an array of 7 washer-stabilized hollow cathode plasma guns [15] which, when electrostatically biased with respect to an external anode, source both plasma and current. The bias on each gun is feedback controlled, allowing current profiles to be tailored in both space and time. The rotating wall itself is a precision-engineered 1 m long by 18 cm diameter stainless steel tube with a 1 mm interior copper liner yielding $\tau_w = 7$ ms. The static wall (vacuum vessel) is also stainless steel with a 0.5 mm exterior copper liner yielding $\tau_w = 4$ ms. The relevant non-dimensional parameter describing rotation is the magnetic Reynolds number ($R_m \equiv \Omega_w \tau_w$, where Ω_w is the wall angular velocity) which

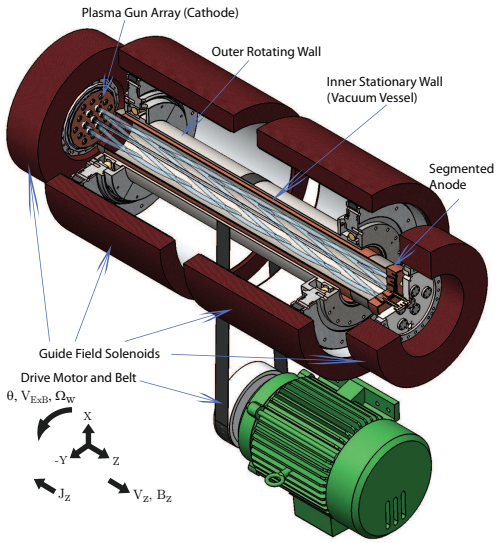

FIG. 1. (Color online) The Rotating Wall Machine [14] experimental geometry. Plasmas are illustrated as discrete flux-ropes though measurements indicate that a fully merged axisymmetric profile is achieved by 1/3rd of the distance to the anode.

sets the ratio of advection to diffusion of the magnetic field. Experiments here described are conducted up to $R_m = 5$, which corresponds to rotation at 260 km/h (6800 RPM). Unless otherwise noted, discharges presented throughout this Letter contain 6 kA of I_p, with the central gun disengaged to generate a less peaked current profile. Langmuir probe measurements [16] indicate the plasma is dense ($n_e \approx 10^{20}$ m^{-3}) and uniformly cold ($T_e \approx$ 3-4 eV), with $n_e \propto I_p$ while T_e is insensitive to I_p. An axial flow ($V_z \approx 8$ km/s, Mach number 0.3) from the guns to the anode has also been measured by a Mach probe [17]. Measurements of MHD activity are made with a low-profile 8 axial by 10 azimuthal B_r edge fluxloop array located in between the static and rotating wall.

Experimental data here presented will be compared to an analytic model for RWM stability in a screw-pinch surrounded by thin walls, as described in Ref. [6]. This ideal MHD model takes the plasma to be force-free, with zero flow, and with a top-hat current profile. The plasma is treated as line-tied at both ends and the the walls are treated by including the effect of wall eddy currents on the perturbed field structure. Stability is calculated by solving the eigenvalue problem for a given plasma radius (r_p) and current (I_p). In this model

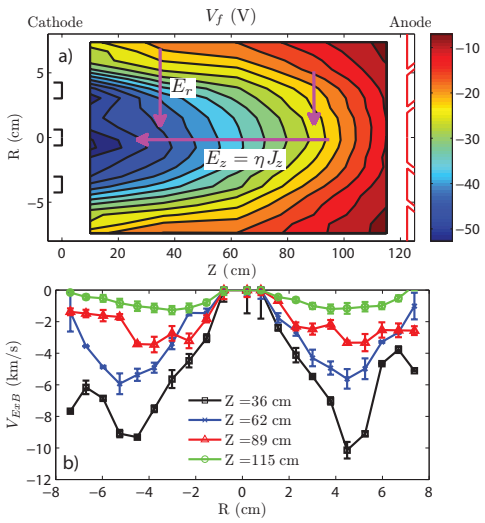

FIG. 2. (Color online) (a) Measurements of floating potential V_f taken at 5 axial by 21 radial equally spaced locations by a single-tip Langmuir probe using shot-to-shot reproducibility. (b) Calculated V_{ExB} flow profiles from (a) at various axial locations illustrating both radial and axial shear. Probe measurements [16] indicate negligible radial current and uniform T_e, justifying this calculation.

the parameter of interest to RWM stability is the safety factor $q(r)$:

$$q(r) = \frac{4\pi^2 r^2 B_z}{\mu_0 I_p(r) L} \tag{1}$$

where L is the device length. As the model current profile is top-hat like, a well-defined r_p exists and stability is uniquely determined by $q(r_p)$. With no rotation, instability to the RWM is found at $q(r_p) < 1$, matching the Kruskal-Shafranov limit [18, 19]. When wall rotation is introduced, the plasma can be stable at $q(r_p) < 1$ and a prediction for the required critical rotation is provided. Coupling to the rotating wall, and thus stabilization, is found to be more effective as r_p approaches r_w. Experimentally, a three-part radially segmented anode provides a coarse measurement of $q(r)$ at $r = 2, 5, 8$ cm as the current within the outer diameter of each anode ring ($I_p(r)$) is known. Previous results [20] have identified the RWM in the device by noting expected scalings of the growth rate with $q(r)$ and τ_w.

Potential gradients, and thus electric fields and ExB flows (shown in Fig. 2) are present in the device due to the large axial bias voltages applied to drive I_p in the relatively cold and resistive plasma. The resulting flow profile is complex, with strong flows near the cathode

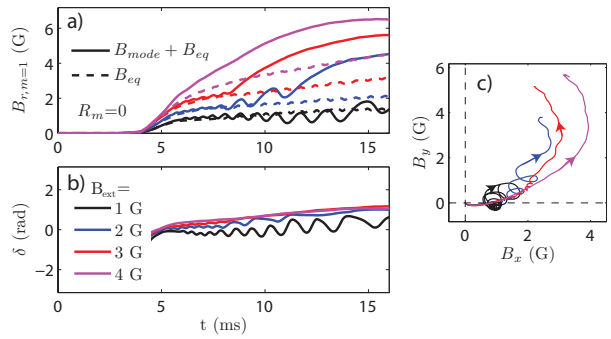

FIG. 3. (Color online) Time-traces of (a) amplitude, (b) phase, (c) hodogram of the $m = 1$ component of B_r with different applied $m = 1$ locking field strengths (B_{ext}). B_{eq} is the plasma equilibrium response to B_{ext}, while B_{ext} is not directly measured as it is applied well-prior to fluxloop integration. B_x and B_y in (c) are the Cartesian projections of the amplitude and phase. For all time-traces in this Letter the discharge begins at $t = 4$ ms.

and vanishing flows near the anode due to the equipotential at the highly conducting surface. MHD modes are thought to take an eigenfunction-weighted average of this flow to set the lab-frame global mode frequency (ω) [17], which is naturally kHz-scale for the experiment. Modes at this frequency are found to be insensitive to wall rotation as $\omega \gg \Omega_w$. Thus, this intrinsic rotation must first be reduced in order to study the effect of the rotating wall on RWM stability. In the torus, this corresponds to slowing toroidal rotation as opposed to azimuthal rotation.

Applying an $m = 1$ error field (B_{ext}) along with increasing guide field ripple ($\tilde{B}_z \approx 1\%$) is found to brake the intrinsic plasma rotation, allowing the RWM (B_{mode}) to lock and grow beyond the equilibrium field (B_{eq}) as shown in Fig. 3. B_{ext}, B_z, and $\tilde{B}_z$ are not directly measured by the fluxloop array as they are applied well prior to plasma formation and fluxloop integration. However, B_{ext} forces the resulting equilibrium to be centered off-axis, thus causing an $m = 1$ component to B_{eq} that is detected. Displayed traces of B_{eq} throughout this Letter are experimentally obtained by minimizing $\tilde{B}_z$ such that the mode rotates very quickly (kHz scale, irrespective of B_{ext}). B_{mode} is thus shielded from the fluxloop array by the static conducting wall and only B_{eq} is measured. A critical $B_{ext} \approx 1.5$ G is necessary to transition the mode from a rotating to a locked RWM, although this value varies with I_p and $\tilde{B}_z$. For $B_{ext} > 3$ G, the observed signal immediately deviates from B_{eq}

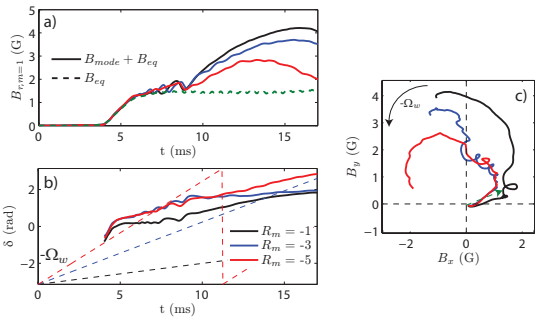

FIG. 4. (Color online) Time-traces of (a) amplitude, (b) phase, (c) hodogram of the $m = 1$ component of B_r at different wall rotation rates (R_m), while holding B_{ext} and B_{eq} constant. Dotted lines in (b) indicate the rate of wall rotation. +ve Ω_w (and +ve R_m) is defined to be co-aligned with the initial plasma ExB rotation throughout this Letter.

and fast mode rotation is never observed, a regime which is termed born-locked. Hodograms (Fig. 3c) clearly illustrate the greatly reduced (though non-zero) ω once locking occurs. It is thought that B_{ext} damps azimuthal rotation primarily through the eletromagnetic torque [21], though changes in viscous torques may also be important and are the object of further study. The role of end-effects in the torque balance is also not yet fully understood. Notwithstanding, mode locking is observed to be abrupt, qualitatively consistent with a recent bifurcation model [22] due to non-monotonic electromagnetic torques. Growth rates of the locked modes are inconsistent with exponential growth, precluding quantitative comparison with theoretical predictions.

Stabilization of the RWM at large R_m is clearly demonstrated for discharges which lock during the discharge lifetime, shown in Fig. 4. Increasing R_m both reduces the growth rate of B_{mode} from the B_{eq} baseline and imparts rotation (ω) to the locked mode, as predicted by theory [6]. For the largest R_m, B_{eq} itself couples to Ω_w and begins to rotate despite arising from a static B_{ext}, as seen in Fig. 4b from 6 to 9 ms. This measurement requires maintaining B_{ext} constant across discharges at varying R_m despite the natural shielding effect of the fast moving wall. This is accomplished by using progressively larger currents to establish the same B_{ext} inside the rotating wall as R_m is increased. Holding this coil current constant while increasing R_m would attenuate B_{ext} and allow the RWM to rotate freely as would be expected by Fig. 3, illustrating another (though indirect) dimension of

RWM stabilization by Ω_w.

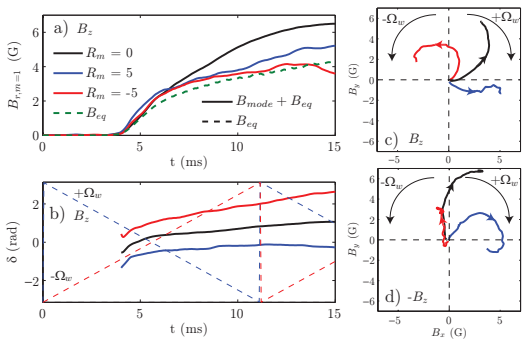

FIG. 5. (Color online) Time-traces of locked-mode (a) amplitude, (b) phase, (c) hodogram of the $m = 1$ component of B_r at different wall rotation rates (R_m), while holding B_{ext} and B_{eq} constant. Dotted lines in (b) indicate the rate of wall rotation. (d) Hodogram at similar R_m, B_{eq}, and B_{ext} though with B_z reversed.

Locking of the RWM to Ω_w is found to be asymmetric in wall rotation direction. Inspection of Fig. 3c illustrates that even in the $R_m = 0$ case a low level residual mode rotation remains whose direction is opposite to the initial plasma ExB rotation. This requires an additional anomalous torque (T_{anom}) which does not vanish when $\omega = 0$. Fig. 5 illustrates the consequences of T_{anom}: wall rotation with Ω_w counter-aligned to T_{anom} decreases the residual rotation, yielding mode-locking to the static wall (vacuum vessel). Discharges with Ω_w co-aligned to T_{anom} increases the residual rotation, bringing ω closer to Ω_w. Reversing B_z is found to reverse this asymmetry (shown in Fig. 5d). Despite the asymmetry in rotation, reductions in the growth rate and mode amplitude are seen in both directions.

Fig. 6 illustrates that $|R_m| > 0$ operation increases the window of RWM-stable operation, as predicted by theory [6]. It is also found that the stabilizing effect is relatively modest until high R_m is achieved. Experiments are done at constant B_z and B_{ext}, such that RWM onset is found as I_p is increased ($q(r)$ decreased). Born-locked modes (largest amplitude traces of Fig. 3) are used to avoid confusion between locking thresholds and RWM onset conditions. Onset is determined by noting where $B_{mode} + B_{eq}$ diverges from the B_{eq} baseline, as shown in Fig. 6a,b. Fig. 6c illustrates the residual B_{mode} amplitude, with higher R_m

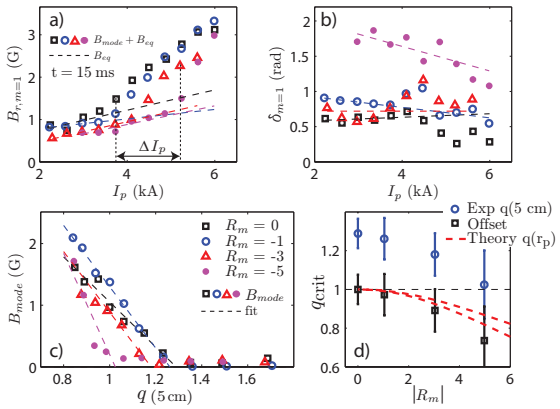

FIG. 6. (Color online) (a) $B_{r,m=1}$ amplitude diverges from B_{eq} at a critical I_p which is raised as R_m increases. (b) Phases of B_{mode} + B_{eq} also vary as I_p increases. (c) B_{mode} amplitude as a function of q as measured by the anode ring at $r = 5$ cm. (d) Comparison of experimental data and theoretical predictions of the critical q (q_{crit}) for instability . The squares in (d) have been offset such that $q_{crit} = 1$ for $R_m = 0$.

operation yielding mode onset at lower $q(r)$ as measured by the 5 cm radius anode ring. Fig. 6d compares experimental and theoretical critical q for instability (q_{crit}). Experimental q_{crit} data is obtained from the zero-crossing of the fits in Fig. 6c, with errors derived from this fit. Theoretical curves are directly calculated from Eq. 54 of Ref. [6] taking $r_p = 6.5$, 7.5 cm (upper, lower curve). The model q profile is constant for $r < r_p$. The experimental q_{crit} is larger than the theoretical prediction for all R_m, as will be later discussed. Offsetting the experimental data such that $q_{crit} = 1$ when $R_m = 0$, the change in q_{crit} as $|R_m|$ increases ($\equiv \Delta q_{crit}$) is found to be in agreement with theory. Furthermore, although $q(5$ cm) has decreased by $\approx 25\%$ ($I_p(5$ cm) increased by $\approx 25\%$), total current ΔI_p has increased by $\approx 40\%$ as shown in Fig. 6a. Larger I_p plasmas are thus less peaked and have a larger plasma radius r_p, providing a second-order stabilizing effect.

Experimental RWM eigenfunctions (shown in Fig. 7) are found to be anode localized in contrast to theoretical predictions (Eq. 27 in Ref. [6]). It is believed that significant axial flows measured in the device [17] are advecting the RWM eigenfunction away from the device midplane, an effect predicted by theory [23] (though not included in Ref. [6]). Additionally, the large sheared azimuthal flows in the cathode region (shown in Fig. 2) are

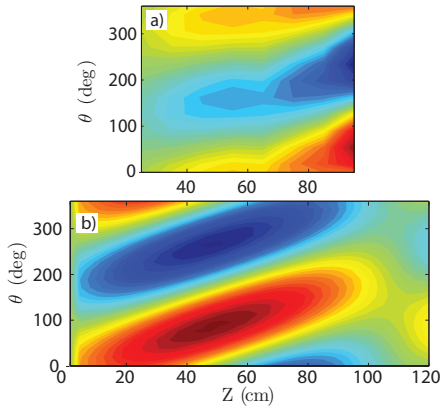

FIG. 7. (Color online) Contour maps of (a) experimental vs (b) theoretical mode eigenfunctions as measured by the B_r fluxloop array. Distances are measured from the cathode while the anode (not shown) is at Z = 123 cm. The smaller size of (a) reflects the axial extent of the fluxloop array.

speculated to be stabilizing the instability in this region. Structure in the cathode (Z $<$ 60 cm) side of Fig. 7a is without helicity and is dominated by B_{eq}.

This experiment has shown qualitative agreement with the theory of Ref. [6], with wall rotation increasing the RWM stability window, decreasing the mode growth rate, and imparting rotation to the RWM. Notwithstanding, several discrepancies remain. Exponential growth is not observed, likely due to the inherent non-linearities present in mode-locking phenomena. The neglected effect of plasma flow is also thought to be the cause of the anode localization of the RWM eigenfunction, the residual locked mode rotation, and the subsequent asymmetry in wall rotation direction seen in experiment. Further, although Δq_{crit} is found to be in agreement, q_{crit} is measured to be larger in experiment (q(5 cm)= 1.3) than in theory ($q(r_p) = 1.0$). However, as the experimental current profile does not resemble the top-hat model [14, 17], a more accurate treatment of the current profile is likely required to reach better agreement. Effects neglected in the plasma model may also account for the discrepancy, such as plasma flows and flow shear, resistivity, and finite pressure. Experimentally, the coarseness of the $q(r)$ measurement also introduces uncertainty, as would any axial variation in the current profile.

This work is supported by Department of Energy grants #DE-FG02-00ER54603 and

#DE-FG02-86ER53218 and National Science Foundation grant #0903900. We also wish to acknowledge the several individuals from the University of Wisconsin Plasma Physics Group and Center for Magnetic Self-Organization (CMSO) who have provided their guidance, support, and time to realizing this effort.

---

* pazsoldan@wisc.edu

[1] M. S. Chu and M. Okabayashi, Plasma Phys. Contr. F. **52**, 123001 (2010), and references therein.

[2] A. Bondeson and D. J. Ward, Phys. Rev. Lett. **72**, 2709 (1994).

[3] C. G. Gimblett, Plasma Phys. Contr. F. **31**, 2183 (1989).

[4] C. G. Gimblett and R. J. Hastie, Phys. Plasmas **7**, 5007 (2000).

[5] M. V. Umansky, R. Betti, and J. P. Freidberg, Phys. Plasmas **8**, 4427 (2001).

[6] C. C. Hegna, Phys. Plasmas **11**, 4230 (2004).

[7] A. M. Garofalo *et al.*, Phys. Rev. Lett. **82**, 3811 (1999).

[8] M. Okabayashi *et al.*, Phys. Plasmas. **8**, 2071 (2001).

[9] P. R. Brunsell *et al.*, Phys. Rev. Lett. **93**, 225001 (2004).

[10] S. A. Sabbagh *et al.*, Phys. Rev. Lett. **97**, 045004 (2006).

[11] J. Rice *et al.*, Nucl. Fusion **47**, 1618 (2007).

[12] R. Fitzpatrick and T. H. Jensen, Phys. Plasmas **3**, 2641 (1996).

[13] S. I. Krasheninnikov, L. E. Zakharov, and G. V. Pereverzev, Phys. Plasmas **10**, 1678 (2003).

[14] C. Paz-Soldan, W. F. Bergerson, M. I. Brookhart, D. A. Hannum, R. Kendrick, G. Fiksel, and C. B. Forest, Rev. Sci. Instrum. **81**, 123503 (2010).

[15] G. Fiksel, A. F. Almagri, D. Craig, M. Iida, S. C. Prager, and J. S. Sarff, Plasma Sources Sci. T. **5**, 78 (1996).

[16] D. Hannum, *Ph.D. Thesis*, University of Wisconsin-Madison, Madison, WI (2010).

[17] C. Paz-Soldan, M. I. Brookhart, A. J. Clinch, D. A. Hannum, and C. B. Forest, Phys. Plasmas **18**, 052114 (2011).

[18] M. Kruskal and M. Schwarzschild, P. R. Soc. A. **223**, 348 (1954).

[19] V. Shafranov, At. Energy (Sov. J. At. Energy) **5**, 38 (1954).

[20] W. F. Bergerson, D. A. Hannum, C. C. Hegna, R. D. Kendrick, J. S. Sarff, and C. B. Forest,

Phys. Rev. Lett. **101**, 235005 (2008).

[21] I. H. Hutchinson, Plasma Phys. Contr. F. **43**, 145 (2001).

[22] E. J. Strait *et al.*, Phys. Plasmas **14**, 056101 (2007).

[23] D. D. Ryutov, I. Furno, T. P. Intrator, S. Abbate, and T. Madziwa-Nussinov, Phys. Plasmas **13**, 032105 (2006).